

Cite this: *Chem. Sci.*, 2025, 16, 20376

All publication charges for this article have been paid for by the Royal Society of Chemistry

# Gram-scale synthesis of (+)-elacestrant streamlined by iridium-catalyzed dynamic kinetic asymmetric hydrogenation of $\alpha$ -substituted tetralones

Yan Zong,<sup>†\*ab</sup> Xiaomei Zou,<sup>†c</sup> Shaoke Zhang,<sup>†a</sup> Gen-Qiang Chen<sup>ID</sup><sup>\*a</sup> and Xumu Zhang<sup>ID</sup><sup>\*a</sup>

A catalytic protocol for the iridium-catalyzed dynamic kinetic resolution asymmetric hydrogenation (DKR-AH) of  $\alpha$ -substituted tetralones to rapidly assemble various enantioenriched tetrahydronaphthols is disclosed. A wide range of enantioenriched tetrahydronaphthols were obtained in high yields and excellent stereoselectivities (up to 99% yield, up to >99.5 : 0.5 er and >20 : 1 dr). And this unique platform exhibited high efficiency for the enantioselective synthesis of (+)-elacestrant, which was approved by the FDA in 2023 for the treatment of metastatic breast cancer. Additionally, palladium-catalyzed amination of aryl chloride assisted in furnishing the gram-scale synthesis of this oral anti-tumor drug within 7 steps in 43% yield.

Received 23rd July 2025  
Accepted 15th September 2025

DOI: 10.1039/d5sc05497d

rsc.li/chemical-science

## Introduction

Breast cancer has overtaken lung cancer as the most frequently diagnosed cancer worldwide, representing the leading health threat to women.<sup>1</sup> Elacestrant (Orserdu, **1**), as the first non-steroidal orally bioavailable selective estrogen receptor degrader (SERD) for the treatment of metastatic breast cancer, was approved by the FDA in 2023 (Fig. 1).<sup>2</sup> The first-year sales of elacestrant have reached 175 million dollars, demonstrating a huge market demand of **1**. Hence, exploration of an efficient route to access elacestrant (**1**) is of great significance.

Elacestrant (**1**) has drawn considerable attention from pharmaceutical companies as well as chemists due to its

excellent therapeutic effects and huge market demand. The general strategies to access elacestrant (**1**) are depicted in Fig. 2A.<sup>3</sup> The vinyl bromide was accessed from 1-tetralone after a three-step manipulation, which was then coupled with *N*-containing aryl bromide *via* a Miyaura borylation/Suzuki coupling sequence. The chirality of this molecule was further

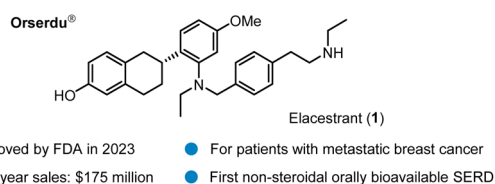


Fig. 1 General information of elacestrant.

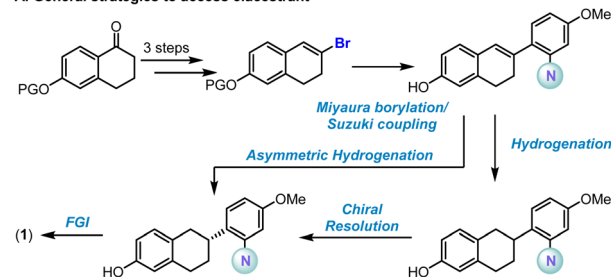
<sup>a</sup>Department of Chemistry, Shenzhen Grubbs Institute, Shenzhen Key Laboratory of Small Molecule Drug Discovery and Synthesis, and Medi-Pingshan, Southern University of Science and Technology, Shenzhen, 518000, China. E-mail: zhangxm@sustech.edu.cn; chengq@sustech.edu.cn; zongy@sustech.edu.cn

<sup>b</sup>Department of Natural Products Chemistry, Key Lab of Chemical Biology, School of Pharmaceutical Sciences, Shandong University, Jinan, 250012, China

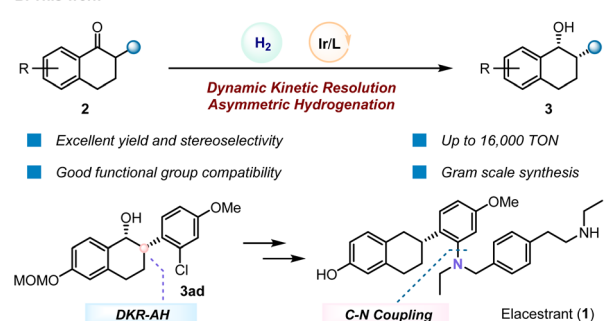
<sup>c</sup>Medical School, Shandong Xiehe University, Jinan, 250109, China

† Yan Zong, Xiaomei Zou, and Shaoke Zhang contributed equally to this work.

### A. General strategies to access elacestrant



### B. This work

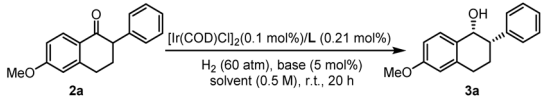
Fig. 2 (A) General strategies to access elacestrant (**1**); (B) enantioselective synthesis of **1** by DKR-AH of  $\alpha$ -substituted tetralones (this work).

introduced *via* chiral resolution of the hydrogenated racemic product or potentially utilizing the asymmetric hydrogenation (AH) of the unfunctionalized alkene.<sup>4</sup> And the final elacestrant (**1**) could be obtained after *N*-alkylation or reductive amination. Nevertheless, the traditional synthetic methods do not meet the requirements of step economy and atom economy since a lengthy step was required to access the Suzuki coupling product, and the chiral resolution gives 50% yield at most. In contrast, dynamic kinetic resolution (DKR) represents a more economical and practical method.<sup>5</sup> We envisioned that the desired chiral center of **1** could be established *via*  $\alpha$ -arylation of 1-tetralone followed by a DKR-AH process to give **3ad**, which was further coupled with the amine part to furnish **1** (Fig. 2B). Although great efforts have been made for transition metal-catalyzed AH<sup>6</sup> or ATH<sup>7</sup> (asymmetric transfer hydrogenation) to achieve this goal, the high catalyst loading (S/C = 1,000 at most) of these methods limited the utilization for the scalable synthesis of elacestrant (**1**). Herein, we report a highly efficient protocol for the DKR-AH of  $\alpha$ -substituted tetralones, and a gram-scale enantioselective synthesis of elacestrant (**1**) could thus be realized based on this protocol.

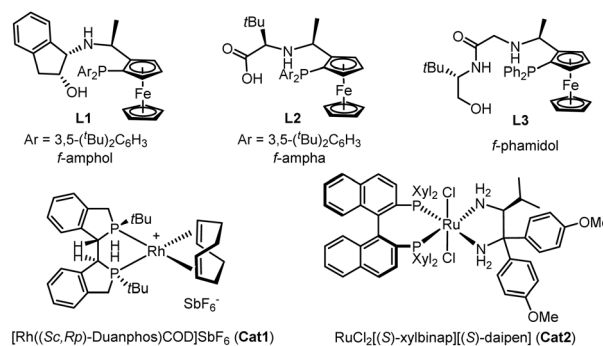
## Results and discussion

Initially, we examined the DKR-AH with **2a** as the model substrate in *i*PrOH, and the results are depicted in Table 1. The ferrocene-based multidentate ligands **L1**<sup>8</sup> and **L2**,<sup>9</sup> which have been demonstrated to show excellent performance for AH of various ketones, were first evaluated, and the desired product **3a** was not detected (Table 1, entries 1 and 2). Delightedly, the reaction proceeded smoothly with the anionic Ir-catalyst with **L3** to give the desired product **3a** with 58% yield, 95.5 : 4.5 er and >20 : 1 dr (Table 1, entry 3).<sup>10</sup> Meanwhile, the frequently used catalysts for the AH of ketones, such as **Cat1**<sup>11</sup> and **Cat2**, were also tested and found to be ineffective with **2a** (Table 1, entries 4 and 5). Then we took our efforts to improve both reactivity and enantioselectivity based on the Ir/**L3** catalytic system. The effect of solvents was examined, and the yield could be dramatically improved to 92% combining with an inconspicuous increase of er with toluene (Table 1, entry 6, 96 : 4 er and >20 : 1 dr). In contrast, other aprotic solvents such as DCM gave inferior results (Table 1, entry 7, 45% yield, 91 : 9 er and >20 : 1 dr). Fortunately, when the reaction was carried out with *tert*-amyl alcohol (*t*AmOH) as solvent, **3a** was obtained with 99% yield, 99 : 1 er and >20 : 1 dr (Table 1, entry 8). And an inconspicuous erosion in reactivity (96% yield, 99 : 1 er and >20 : 1 dr) was obtained with *tert*-butyl alcohol (*t*BuOH) as solvent (Table 1, entry 9). However, diminished yields were obtained when other protic solvents such as MeOH or HFIP were used (Table 1, entries 10 and 11) (for the detailed screening of solvents, see Table S1 in the SI). Based on our previous research experience, the protic solvents generally give better results compared with aprotic solvents, especially at low catalyst loading. The protic solvents such as MeOH and EtOH might undergo dehydrogenation and decarbonylation processes to release CO, which can possibly poison the catalyst.<sup>10a</sup> In this case, the protic solvents *t*BuOH and *t*AmOH could give similarly better results.

Table 1 Reaction condition optimization for DKR-AH of **2a**<sup>a</sup>



Entry	Ligand	Solvent	Base	Yield (%)	Er	Dr
1	<b>L1</b>	<i>i</i> PrOH	<i>t</i> BuONa	3	—	—
2	<b>L2</b>	<i>i</i> PrOH	<i>t</i> BuONa	0	—	—
3	<b>L3</b>	<i>i</i> PrOH	<i>t</i> BuONa	58	95.5 : 4.5	>20 : 1
4 <sup>b</sup>	—	<i>i</i> PrOH	<i>t</i> BuONa	0	—	—
5 <sup>c</sup>	—	<i>i</i> PrOH	<i>t</i> BuONa	0	—	—
6	<b>L3</b>	PhMe	<i>t</i> BuONa	92	96 : 4	>20 : 1
7	<b>L3</b>	DCM	<i>t</i> BuONa	45	91 : 9	>20 : 1
8	<b>L3</b>	<i>t</i> AmOH	<i>t</i> BuONa	99	99 : 1	>20 : 1
9	<b>L3</b>	<i>t</i> BuOH	<i>t</i> BuONa	96	99 : 1	>20 : 1
9	<b>L3</b>	MeOH	<i>t</i> BuONa	0	—	—
10	<b>L3</b>	HFIP	<i>t</i> BuONa	0	—	—
11	<b>L3</b>	<i>t</i> AmOH	<i>t</i> BuOK	60	95 : 5	>20 : 1
12	<b>L3</b>	<i>t</i> AmOH	<i>t</i> BuOLi	20	95 : 5	>20 : 1
13	<b>L3</b>	<i>t</i> AmOH	Na <sub>2</sub> CO <sub>3</sub>	0	—	—
14	<b>L3</b>	<i>t</i> AmOH	NaOH	87	98.5 : 1.5	>20 : 1



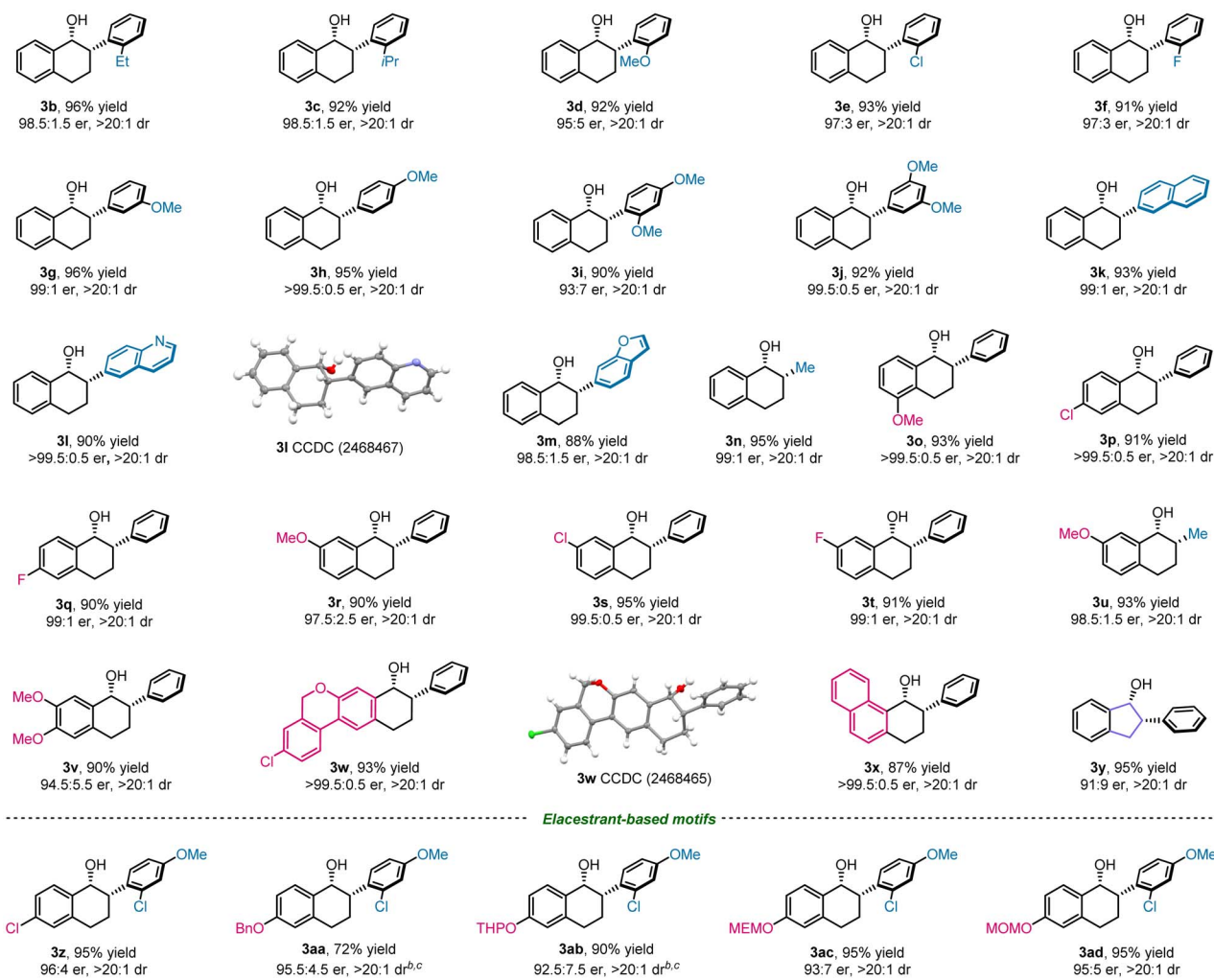
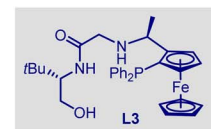
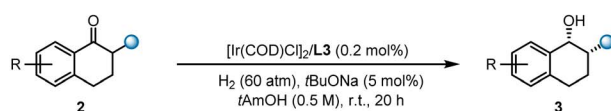
<sup>a</sup> Reaction conditions: all reactions were performed with **2a** (0.2 mmol), **Cat1**, **Cat2** or Ir/**L1–L3** (0.2 mol%), and base (5 mol%) in solvent (0.4 mL) under 60 bar of H<sub>2</sub>, stirred at room temperature for 20 h. Diastereomeric ratios (drs) and yields were determined by <sup>1</sup>H NMR spectroscopy. Enantiomeric ratios (ers) were determined by HPLC. <sup>b</sup> **Cat1** was used as the catalyst. <sup>c</sup> **Cat2** was used as the catalyst.

Compared with *t*BuOH, *t*AmOH has a lower melting point, and the problem of solidification was avoided.

Bases such as *t*BuOK, *t*BuOLi, Na<sub>2</sub>CO<sub>3</sub> and NaOH were also evaluated, and the yields of **3a** were significantly decreased with *t*BuOK or *t*BuOLi as the base, albeit retaining high stereoselectivities (Table 1, entries 12 and 13). Na<sub>2</sub>CO<sub>3</sub> was completely ineffective, probably due to its low basicity (Table 1, entry 14), whereas 87% yield, 98.5 : 1.5 er and >20 : 1 dr were achieved with NaOH as the base (Table 1, entry 15) (for the detailed screening of other bases, see Table S2 in the SI).

With the optimized reaction conditions in hand, we then turned our attention to the investigation of the substrate generality, and variations on the  $\alpha$ -substitution of tetralones were first evaluated. As was shown in Scheme 1, substrates with various substituents at the *ortho*-position of the phenyl group (**2b–2f**) gave excellent yields and high stereoselectivities





**Scheme 1** Substrate scope of the DKR-AH of  $\alpha$ -substituted tetralones. <sup>a</sup>Unless otherwise specified, the reactions were performed with L2 (0.2 mmol), Ir/L3 (0.2 mol%), and *t*BuONa (5 mol%) in *t*AmOH (0.4 mL) under H<sub>2</sub> (60 atm) at room temperature for 20 h. Yields and diastereomeric ratios (drs) were determined by <sup>1</sup>H NMR spectroscopy. Enantiomeric ratios (ers) were determined by HPLC analysis using a chiral stationary phase. <sup>b</sup>20 mol% *t*BuONa was used. <sup>c</sup>Stirred at room temperature for 72 h.

(91–96% yield, 95 : 5–98.5 : 1.5 er and >20 : 1 dr for all cases). The reactions with *meta*- or *para*-substituted methoxy groups and 3,5- or 2,4-di-methoxy substituents on the phenyl group (**2g–2j**) were also investigated, providing the desired products with high yields and excellent stereoselectivities (90–96% yield, 93 : 7–>99.5 : 0.5 er and >20 : 1 dr for all cases). 2-Naphthyl and heterocyclic substrates could deliver the desired products **3k–3m** with 88 to 93% yield, 98.5 : 1.5–>99.5 : 0.5 er and >20 : 1 dr as well. In addition,  $\alpha$ -methyl substituted tetralone (**2n**) was surveyed, providing the desired product in 95% yield, 99 : 1 er and >20 : 1 dr. Identically, a robust reactivity was also found for substrates with different substituents at the 5-, 6- and 7-positions of the tetralone rings, leading to the desired products **3o–**

**3v** in 90–95% yield, 94.5 : 5.5–>99.5 : 0.5 er and >20 : 1 dr. Subsequently, the polycyclic substrates were investigated to be compatible with this catalytic system, giving **3w** and **3x** with excellent results (87–93% yield, >99.5 : 0.5 er and >20 : 1 dr for both cases). Finally, the five-membered substrate **2y** was also surveyed, and the desired product **3y** was obtained in 95% yield and >20 : 1 dr, albeit with erosion of enantioselectivity (91 : 9 er). Additionally, the absolute and relative configuration of this type of products was unambiguously determined by the X-ray crystallographic analysis of **3l** and **3w**.

Before commencing the investigation for the synthesis of **1**, we concentrated our efforts on the DKR-AH of elacestrant-based motifs with substrates bearing various functional groups at the

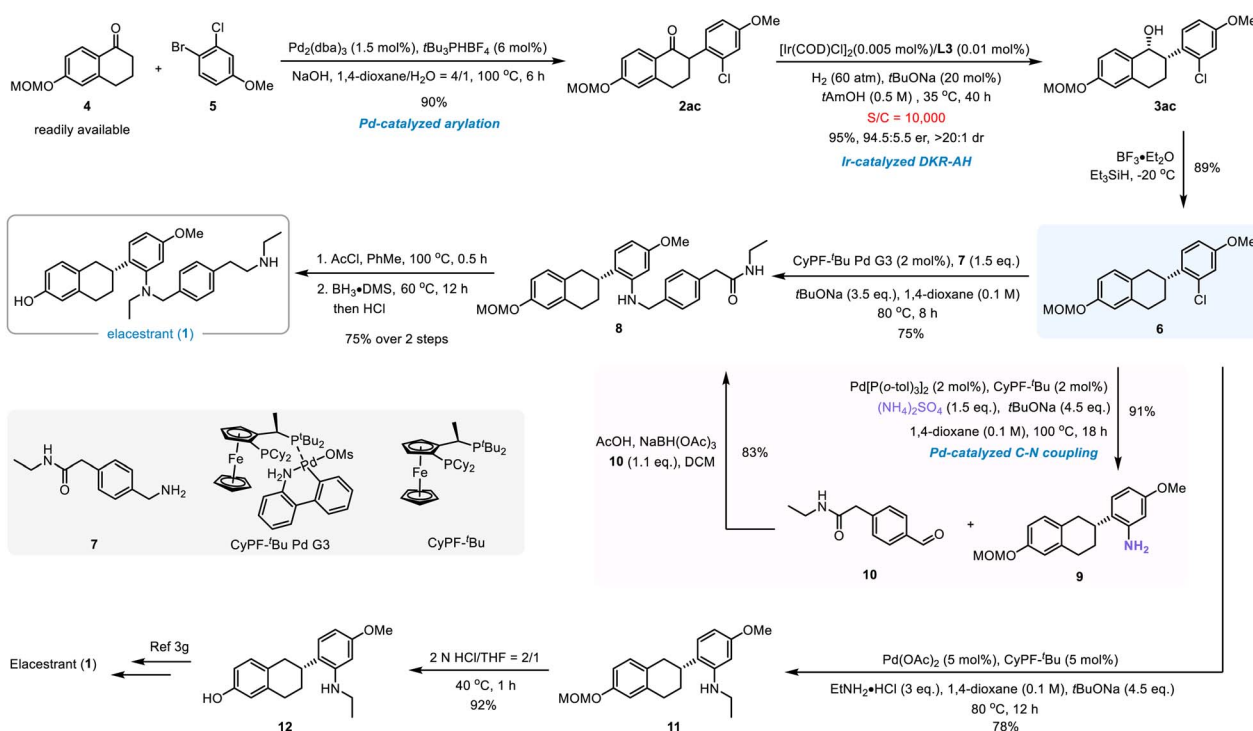


6-position of the tetralone (bottom in Scheme 1). 6-Chloro substituted **2z** was first surveyed, the product of which could be potentially transformed to **1** through a C–O coupling to install the 6-OH,<sup>12</sup> and the desired product **3z** was obtained in 95% yield, 96 : 4 er and >20 : 1 dr. Nevertheless, from the viewpoint of step-economy, using 6-oxygen-containing substrates seemed a more straightforward means. This catalytic system exhibited relatively low reactivity with **2aa** bearing a benzyl group, which was widely used in elacestrant synthesis, providing **3aa** in 72% yield, 95.5 : 4.5 er and >20 : 1 dr. Therefore, we tried to find other suitable phenol protections. Base-sensitive protective groups such as silyl or acyl were not suitable, because they were incompatible with the hot aqueous basic conditions under which the  $\alpha$ -arylation process was conducted. Subsequently, the THP and MEM protective groups were evaluated, and the corresponding products **3ab** and **3ac** were produced in high yields, albeit with slight erosion of enantioselectivities (92.5 : 7.5–93 : 7 er and >20 : 1 dr for both cases). Much to our delight, when the reaction was carried out with **2ad** bearing a MOM group, the desired product was delivered in 95% yield, 95 : 5 er and >20 : 1 dr.

With the key intermediate **3ad** secured, we then concentrated our efforts on the gram-scale enantioselective synthesis of elacestrant (**1**). As was outlined in Scheme 2, **2ad** was delivered in 90% yield when the reaction was carried out under the general palladium-catalyzed  $\alpha$ -arylation conditions with **4** and **5**. Gratifyingly, the gram-scale DKR-AH of substrate **2ad** (2.1 g, 6.1 mmol) proceeded smoothly at 35 °C and in the presence of 20 mol% *t*BuONa to give the desired product **3ad** in 95% yield,

94.5 : 5.5 er and >20 : 1 dr with a substrate-to-catalyst ratio (S/C) of 10,000 (for the detailed TON exploration, see Table S3 in the SI). After reductive deoxygenation with triethylsilane at –20 °C,<sup>13</sup> compound **6** was obtained in 89% yield. Notably, an increased amount of the MOM deprotected byproduct was detected when the reaction was conducted at higher temperatures.

With the key intermediate **6** in hand, we then continued our exploration of the installation of the N-containing moiety. The C–N coupling with amine seemed to be challenging with either palladium- or copper-catalytic systems,<sup>14</sup> possibly due to the low reactivity of aryl chloride as well as the bulkiness of the aryl chloride partner. After many attempts, the desired product **8** could be produced smoothly with amine **7**. Alternatively, the C–N coupling reaction could also proceed smoothly for *ortho*-substituted aryl chloride **6** with inexpensive and easily handled ammonium sulfate,<sup>15</sup> leading to primary aryl amine **9** in 91% yield on a 1.4 g scale with 2 mol% catalyst loading. And the desired product **8** was delivered in high yield *via* reductive amination with a slight excess of **10**. Moving forward, we noted that we were unable to assemble the required acyl group to access the desired tertiary amide fruitfully through direct acylation with general protocols (*e.g.*: AcCl, TEA, DMAP; AcCl, NaH; Ac<sub>2</sub>O, pyridine). Fortunately, the desired secondary amine could be chemoselectively acylated with high efficiency by refluxing **8** with acyl chloride in toluene,<sup>16</sup> and the final elacestrant (**1**) could be obtained in 75% overall yield after global reduction of amides and deprotection of MOM. Notably, the C–N coupling of **6** with ethyl amine according to Hartwig's protocol was also



Scheme 2 Completion of elacestrant (**1**) *via* C–N coupling with various amines.



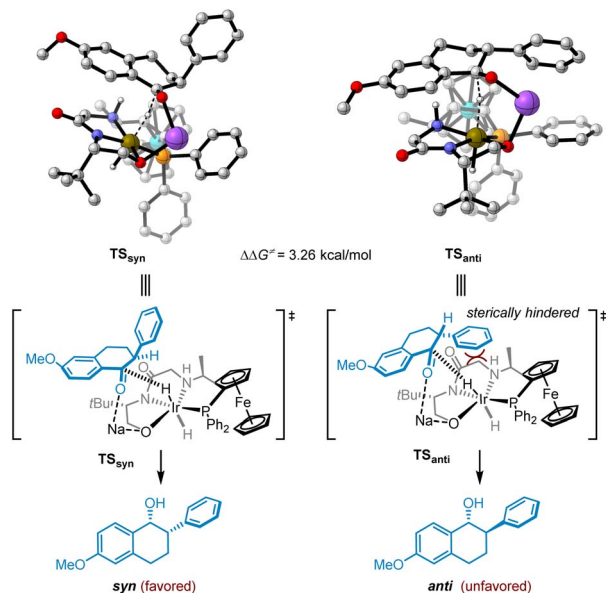


Fig. 3 Calculated transition states for the *syn*- and *anti*-products.

successful,<sup>15</sup> and the reported common intermediate **12** for elacestrant (**1**) was obtained after removal of the MOM protective group.<sup>3g</sup>

The key step of our enantioselective synthesis of elacestrant relies on the excellent enantio- and diastereo-control of the DKR-AH of  $\alpha$ -substituted tetralones. To give a full insight into the origin of high diastereoselectivity, we calculated the transition states leading to the *syn*- and *anti*-products with **2a** as the model substrate. As shown in Fig. 3, the transition state leading to the *anti*-product is energetically less favored due to the steric hindrance between the  $\alpha$ -phenyl substituent and the catalyst, resulting in a 3.26 kcal mol<sup>-1</sup> lower energy of  $TS_{syn}$  compared with  $TS_{anti}$ , which is quantitatively in line with our experimental results.

## Conclusions

In summary, we have successfully developed a highly powerful protocol for the gram-scale enantioselective synthesis of the oral anti-breast cancer drug elacestrant (**1**) within 7 steps in 43% overall yield, which was facilitated by the efficient iridium-catalyzed DKR-AH of  $\alpha$ -substituted tetralones (up to 99% yield, >99.5 : 0.5 er and >20 : 1 dr for all cases) and a late-stage amination with various types of amines. The significance of this method was demonstrated by the construction of the target chirality of **1** with a substrate-to-catalyst (S/C) ratio of 10 000, showing broad potential and prospects for industrial application. The industrial enantioselective synthesis of elacestrant (**1**) with this synthetic route is currently underway in our laboratory and will be reported in due course.

## Author contributions

Yan Zong and Xiaomei Zou carried out the experimental work and wrote the first draft. Xiaomei Zou and Shaoke Zhang performed experimental testing. Gen-Qiang Chen and Xumu Zhang designed the project and supervised the work. All the authors discussed the manuscript.

## Conflicts of interest

There are no conflicts to declare.

## Data availability

The data that support the findings of this study are available from the SI or from the authors upon reasonable request. CCDC 2468465 and 2468467 contain the supplementary crystallographic data for this paper.<sup>17a,b</sup>

Supplementary information: all experimental and characterization data, NMR spectra, crystallographic data of **3l** and **3w** and DFT calculations. See DOI: <https://doi.org/10.1039/d5sc05497d>.

## Acknowledgements

X. Zhang is indebted to the financial support from the National Key R&D Program of China (2021YFA1500200), National Natural Science Foundation of China (no. 21991113), Chemistry and Chemical Engineering Guangdong Laboratory (grant no. 2011006 and 2132013), Shenzhen Key Basic Research Project (JCYJ20241202125305008), High level of special funds (G03050K003) and Innovative Team of Universities in Guangdong Province (no. 2020KCXTD016). G.-Q. Chen gratefully acknowledges the National Natural Science Foundation of China (no. 22171129), Shenzhen Science and Technology Innovation Committee (JCYJ20240813095106009), Guangdong Innovative Program (2019BT02Y335), and Guangdong Basic and Applied Basic Research Foundation (2022B1515020055) for financial support. S. Zhang appreciates the support of the National Natural Science Foundation of China (22302090) and Guangdong Basic and Applied Basic Research Foundation (2022A1515110093).

## Notes and references

- W. Cao, H. Chen, Y. Yu, N. Li and W. Chen, *Chin. Med. J.*, 2021, **134**, 783–791.
- (a) J. H. Beumer and J. Foldi, *Cancer Chemoth. Pharm.*, 2023, **92**, 157–163; (b) S. M. Hoy, *Drugs*, 2023, **83**, 555–561.
- (a) G. Cheng, *China Pat.*, CN116969848, 2023; (b) S. Hamaoka, N. Kitazawa, K. Nara, A. Sasaki, A. Kamada and T. Okabe, WO2004058682, 2004; (c) M. Markey, WO2020167855, 2020; (d) F. Morini, F. Calvani, M. Masi, F. D'Arata, F. Bonaccorsi, A. Ramacciotti and R. Schmitz, WO2025083026, 2025; (e) F. Pan, Y. Yang, C. Shen, M. Liu, X. Liu and D. Wang, *China Pat.*, CN119661379, 2025; (f) Y. Yang, Y. Huang and Y. He, *China Pat.*, CN118791392,



- 2024; (g) Q. Liu, S. Yi, S. Wang, H. Gao, H. Wang and X. Wang, *China Pat.*, CN118702588, 2024.
- 4 (a) T. Pan, Q. Yuan, D. Xu and W. Zhang, *Org. Lett.*, 2024, **26**, 5850–5855; (b) P. Cheruku, A. Paptchikhine, M. Ali, J.-M. Neudörfl and P. G. Andersson, *Org. Biomol. Chem.*, 2008, **6**, 366–373; (c) C. Hedberg, K. Källström, P. Brandt, L. K. Hansen and P. G. Andersson, *J. Am. Chem. Soc.*, 2006, **128**, 2995–3001.
- 5 (a) M.-R. Liang, X. Du, J. Lin, N. Rong, X. Zhan, X. Mao, H. Zhuang, T. Niu and Q. Yin, *J. Am. Chem. Soc.*, 2025, **147**, 4239–4248; (b) R. Liu, X. Ding, Q. Lang, G.-Q. Chen and X. Zhang, *Chin. Chem. Lett.*, 2025, **36**, 110037; (c) J.-Y. Wang, C.-H. Gao, C. Ma, X.-Y. Wu, S.-F. Ni, W. Tan and F. Shi, *Angew. Chem., Int. Ed.*, 2024, **63**, e202316454; (d) P. Wu, L. Yu, C.-H. Gao, Q. Cheng, S. Deng, Y. Jiao, W. Tan and F. Shi, *Fundam. Res.*, 2023, **3**, 237–248; (e) H.-Q. Wang, S.-F. Wu, J.-R. Yang, Y.-C. Zhang and F. Shi, *J. Org. Chem.*, 2023, **88**, 7684–7702; (f) Z. Chen, Y. Aota, H. M. H. Nguyen and V. M. Dong, *Angew. Chem., Int. Ed.*, 2019, **58**, 4705–4709; (g) X. Chen, J. Z. M. Fong, J. Xu, C. Mou, Y. Lu, S. Yang, B.-A. Song and Y. R. Chi, *J. Am. Chem. Soc.*, 2016, **138**, 7212–7215.
- 6 (a) J. Li, J. Ye, J. Zhou, J. Li, D. Liu and W. Zhang, *Chem. Commun.*, 2022, **58**, 4905–4908; (b) O. V. Zatolochnaya, S. Rodriguez, Y. Zhang, K. S. Lao, S. Tcyrulnikov, G. Li, X.-J. Wang, B. Qu, S. Biswas, H. P. R. Mangunuru, D. Rivalenti, J. D. Sieber, J.-N. Desrosiers, J. C. Leung, N. Grinberg, H. Lee, N. Haddad, N. K. Yee, J. J. Song, M. C. Kozlowski and C. H. Senanayake, *Chem. Sci.*, 2018, **9**, 4505–4510.
- 7 (a) T. Touge, K. Sakaguchi, N. Tamaki, H. Nara, T. Yokozawa, K. Matsumura and Y. Kayaki, *J. Am. Chem. Soc.*, 2019, **141**, 16354–16361; (b) F. Wang, T. Yang, T. Wu, L.-S. Zheng, C. Yin, Y. Shi, X.-Y. Ye, G.-Q. Chen and X. Zhang, *J. Am. Chem. Soc.*, 2021, **143**, 2477–2483; (c) W. Ye, Q. An, D. Gou, Q. Zhang, Y. Xu and J. Wang, *China Pat.*, CN119751274, 2025.
- 8 (a) L. Tao, C. Yin, X.-Q. Dong and X. Zhang, *Org. Biomol. Chem.*, 2019, **17**, 785–788; (b) C. Yin, X.-Q. Dong and X. Zhang, *Adv. Synth. Catal.*, 2018, **360**, 4319–4324; (c) J. Yu, M. Duan, W. Wu, X. Qi, P. Xue, Y. Lan, X.-Q. Dong and X. Zhang, *Chem. Eur. J.*, 2017, **23**, 970–975.
- 9 (a) G. Gu, T. Yang, J. Lu, J. Wen, L. Dang and X. Zhang, *Org. Chem. Front.*, 2018, **5**, 1209–1212; (b) W. Li, T. Yang, N. Song, R. Li, J. Long, L. He, X. Zhang and H. Lv, *Chem. Sci.*, 2022, **13**, 1808–1814; (c) J. Yu, J. Long, Y. Yang, W. Wu, P. Xue, L. W. Chung, X.-Q. Dong and X. Zhang, *Org. Lett.*, 2017, **19**, 690–693.
- 10 (a) C. Yin, Y. F. Jiang, F. Huang, C. Q. Xu, Y. Pan, S. Gao, G. Q. Chen, X. Ding, S. T. Bai, Q. Lang, J. Li and X. Zhang, *Nat. Commun.*, 2023, **14**, 3718; (b) J. Yu, F. Huang, W. Fang, C. Yin, C. Shi, Q. Lang, G.-Q. Chen and X. Zhang, *Green Synth. Catal.*, 2022, **3**, 175–178; (c) Y. Zong, X. Zou, J. Song, G.-Q. Chen and X. Zhang, *Org. Lett.*, 2023, **25**, 6875–6880; (d) Y. e. You, C. Yin, L. Xu, G.-Q. Chen and X. Zhang, *Green Synth. Catal.*, 2024, **5**, 141–152.
- 11 (a) D. Liu, W. Gao, C. Wang and X. Zhang, *Angew. Chem., Int. Ed.*, 2005, **44**, 1687–1689; (b) Y. Zong, S. Gao, X. Zou, Q. Huang, G.-Q. Chen and X. Zhang, *Chin. J. Chem.*, 2025, **43**, 1783–1788.
- 12 (a) Z. Chen, Y. Jiang, L. Zhang, Y. Guo and D. Ma, *J. Am. Chem. Soc.*, 2019, **141**, 3541–3549; (b) S. Xia, L. Gan, K. Wang, Z. Li and D. Ma, *J. Am. Chem. Soc.*, 2016, **138**, 13493–13496.
- 13 W.-X. Xu, Z. Peng, Q.-X. Gu, Y. Zhu, L.-H. Zhao, F. Leng and H.-H. Lu, *Nat. Synth.*, 2024, **3**, 986–997.
- 14 (a) D. Maiti, B. P. Fors, J. L. Henderson, Y. Nakamura and S. L. Buchwald, *Chem. Sci.*, 2011, **2**, 57–68; (b) W. Zhou, M. Fan, J. Yin, Y. Jiang and D. Ma, *J. Am. Chem. Soc.*, 2015, **137**, 11942–11945.
- 15 R. A. Green and J. F. Hartwig, *Org. Lett.*, 2014, **16**, 4388–4391.
- 16 K. Tsuboi, D. A. Bachovchin, A. E. Speers, T. P. Spicer, V. Fernandez-Vega, P. Hodder, H. Rosen and B. F. Cravatt, *J. Am. Chem. Soc.*, 2011, **133**, 16605–16616.
- 17 (a) Y. Zong, X. Zou, S. Zhang, G.-Q. Chen and X. Zhang, CCDC 2468465: Experimental Crystal Structure Determination, 2025, DOI: [10.5517/ccdc.csd.cc2nvmx2](https://doi.org/10.5517/ccdc.csd.cc2nvmx2); (b) Y. Zong, X. Zou, S. Zhang, G.-Q. Chen and X. Zhang, CCDC 2468467: Experimental Crystal Structure Determination, 2025, DOI: [10.5517/ccdc.csd.cc2nvmz4](https://doi.org/10.5517/ccdc.csd.cc2nvmz4).

